Electronic Supplementary Material (ESI) for Polymer Chemistry.
This journal is © The Royal Society of Chemistry 2019

Supporting Information for:

Synthesis of Block Copolymer Nano-assemblies via ICAR ATRP dispersion polymerization: How ATRP and RAFT lead to difference

Shuwen Qu,‡[a] Ke Wang,‡[a] Habib Khan,[a] Weifeng Xiong,*[b] and Wangqing Zhang*[a,c]

[a] Key Laboratory of Functional Polymer Materials of the Ministry of Education, Institute of Polymer Chemistry, Nankai University, Tianjin 300071, China.

[b] State Key Laboratory of Special Functional Waterproof Materials, Beijing Oriental Yuhong Waterproof Technology Co., Ltd, Beijing 100123, China.

[c] Collaborative Innovation Center of Chemical Science and Engineering (Tianjin), Nankai University, Tianjin 300071, China.

* To whom correspondence should be addressed. E-mail: (W. X.) xiongwf@yuhong.com.cn. (W. Z.) wqzhang@nankai.edu.cn. Tel: (W. Z.) 0086-22-23509794.

‡ These authors contributed equally to this manuscript.

1. Synthesis of PEG_{45}-Br, PEG_{45}-TTC

2-Bromoisobutyryl-terminated poly(ethylene glycol) monomethyl ether (PEG_{45}-Br) was synthesized as follows. CH_3O-PEG_{45}-OH (10.0 g, 5.0 mmol) was dissolved in 300 mL anhydrous toluene in a 500 mL flask. After azeotropic distillation to remove traces of water, trimethylamine (1.4 mL, 10 mmol) was added, and the mixture was cooled to 0 ℃. Then, 2-bromoisobutyryl bromide (1.2 mL, 10 mmol) was added via syringe over 1 hour. The reaction mixture was stirred overnight at room temperature and washed with saturated sodium bicarbonate solution. The aqueous phase was extracted with CH_2Cl_2 and organic layers were collected. The concentrated organic layers were precipitated in diethyl ether and dried under reduced pressure.

Trithiocarbonate-terminated poly(ethylene glycol) monomethyl ether (PEG_{45}-TTC) is synthesized as follows. DDMAT (3.36 g, 10.0 mmol) and CH_2Cl_2 (50.0 mL) were added in a dry flask. Into the flask, a mixture of $(COCl)_2$ (4.2 mL,

25.0 mmol) and CH_2Cl_2 (20.0 mL) was added dropwise under nitrogen atmosphere at room temperature for about 4 h, then the excess oxalyl chloride was removed by rotary evaporation. CH_3O-PEG_{45}-OH (10.0 g, 5.0 mmol) dissolved in CH_2Cl_2 (50 mL) was added under nitrogen atmosphere, the reaction was conducted at room temperature for 24 h. After concentrated on a rotary evaporator, PEG_{45}-TTC was precipitated in n-hexane and dried under reduced pressure.

2. Monomer conversion of styrene analyzed by UV-vis spectroscopy

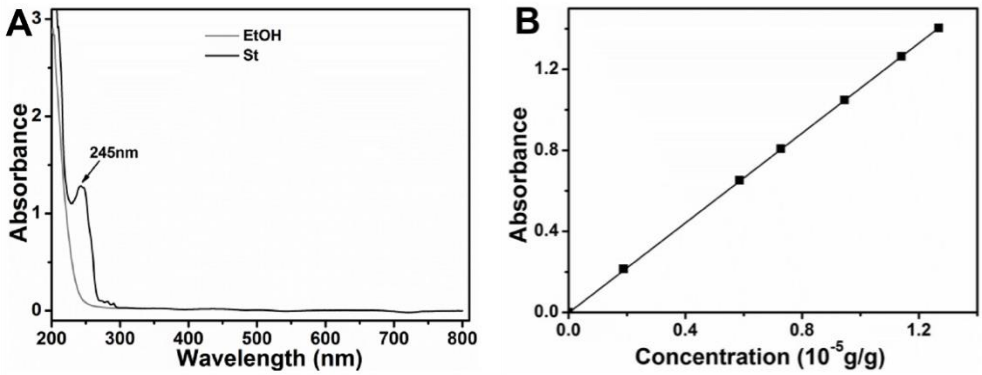

Figure S1. UV -vis absorption spectra of the solvent of ethanol and the ethanol solution of styrene (A) and the absorbance of styrene at 245 nm at different concentration of styrene in ethanol (B).

The monomer conversion of styrene is measured as follows.The polymerization was quenched by immersing the flask in iced water. The monomer conversion was detected by UV–vis analysis, in which a given volume of the colloidal dispersion solution (ca. 1.0 mL) was filtrated twice with a 0.22-μm nylon filter, and then the filtrate was diluted with ethanol and analyzed at 245 nm. The amount of residual styrene in the reaction solution can be obtained by comparing the measured absorption coefficient with the standard curve as shown in Figure S1

3. Synthesis of BCP nano-assemblies by ICAR ATRP dispersion polymerization

The theoretical molecular weight is calculated by the following equation:

$$M_{n,th} = \frac{[\text{monomer}]_0 \times M_{\text{monomer}}}{[\text{Macroinitiator}]_0} \times Conversion + M_{\text{n,Macroinitiator}} \quad (S1)$$

Table S1. Block copolymers synthesized by ICAR ATRP dispersion polymerization.

Entry	polymer	Temp (℃)	x	Time (h)	Conv. (%)[a]	M_n (kg/mol)			$Đ$[e]
						$M_{n,th}$[b]	$M_{n,GPC}$[c]	$M_{n,NMR}$[d]	
1	PEG_{45}-*b*-PS_{106}	45	2	6	35.2	13.2	11.7	18.6	1.48
2	PEG_{45}-*b*-PS_{187}	45	3	6	62.3	21.5	15.6	27.3	1.72
3	PEG_{45}-*b*-PS_{217}	45	4	6	72.2	24.7	13.8	29.5	1.68
4	PEG_{45}-*b*-PS_{218}	45	5	6	72.6	24.8	11.4	29.8	1.53
5	PEG_{45}-*b*-PS_{221}	45	6	6	73.8	25.1	10.5	34.2	1.40
6	PEG_{45}-*b*-PS_{226}	45	7	6	75.4	25.6	9.8	34.6	1.37
7	PEG_{45}-*b*-PS_{233}	45	8	6	77.7	26.3	9.6	35.1	1.33
8	PEG_{45}-*b*-PS_{108}	40	6	6	36.3	13.5	7.2	19.3	1.25
9	PEG_{45}-*b*-PS_{263}	50	6	6	87.8	29.5	8.6	38.9	1.38
10	PEG_{45}-*b*-$PMMA_{296}$	45	6	4	98.5%	32.1	28.8	32.4	1.21
11	$PHPMA_{29}$-*b*-$PMMA_{295}$	45	6	4	98.2%	34.3	48.5	---	1.51
12	$PHPMA_{29}$-*b*-$BzMA_{300}$	45	6	3	99.9%	57.3	68.3	63.5	1.38

[a] The monomer conversion determined by ^{1}H NMR analysis. [b] Theoretical molecular weight according to eq S1. [c] Molecular weight determined by GPC analysis. [d] Molecular weight determined by ^{1}H NMR analysis. [e] The $Đ$ (M_w/M_n) values determined by GPC analysis. Polymerization conditions: $[St]_0$:$[PEG\text{-}Br]_0$:$[Cu^{II}Br_2]_0$:$[TPMA]_0$:$[VA\text{-}044]_0$ = 300:1:0.1x:0.4x:1.0x, 20 wt% solid content in the 80/20 MeOH/H_2O mixture (Entry 1-9); $[monomer]_0$:$[macroinitiator]_0$:$[Cu^{II}Br_2]_0$:$[TPMA]_0$:$[VA\text{-}044]_0$ = 300:1:0.6:2.4:6, 20 wt% solid content in the 40/60 MeOH/H_2O mixture (Entry 10), in the 60/40 MeOH/H_2O mixture (Entry 11) and in the 80/20 MeOH/H_2O mixture (Entry 12).

4. Characterization of PEG_{45}-*b*-PS by ICAR ATRP dispersion polymerization

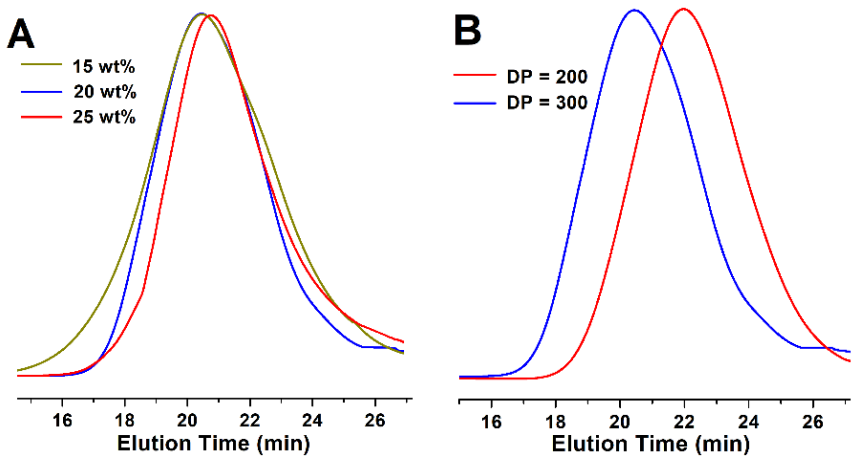

Figure S2. GPC traces of PEG_{45}-*b*-PS synthesized at same targeted DP of PS block but different solid content (A) and at 20 wt% solid content but with different targeted DP (B) of the PS block by ICAR ATRP dispersion polymerization.

5. Synthesis and characterization of PEG_{45}-*b*-PS by RAFT dispersion polymerization

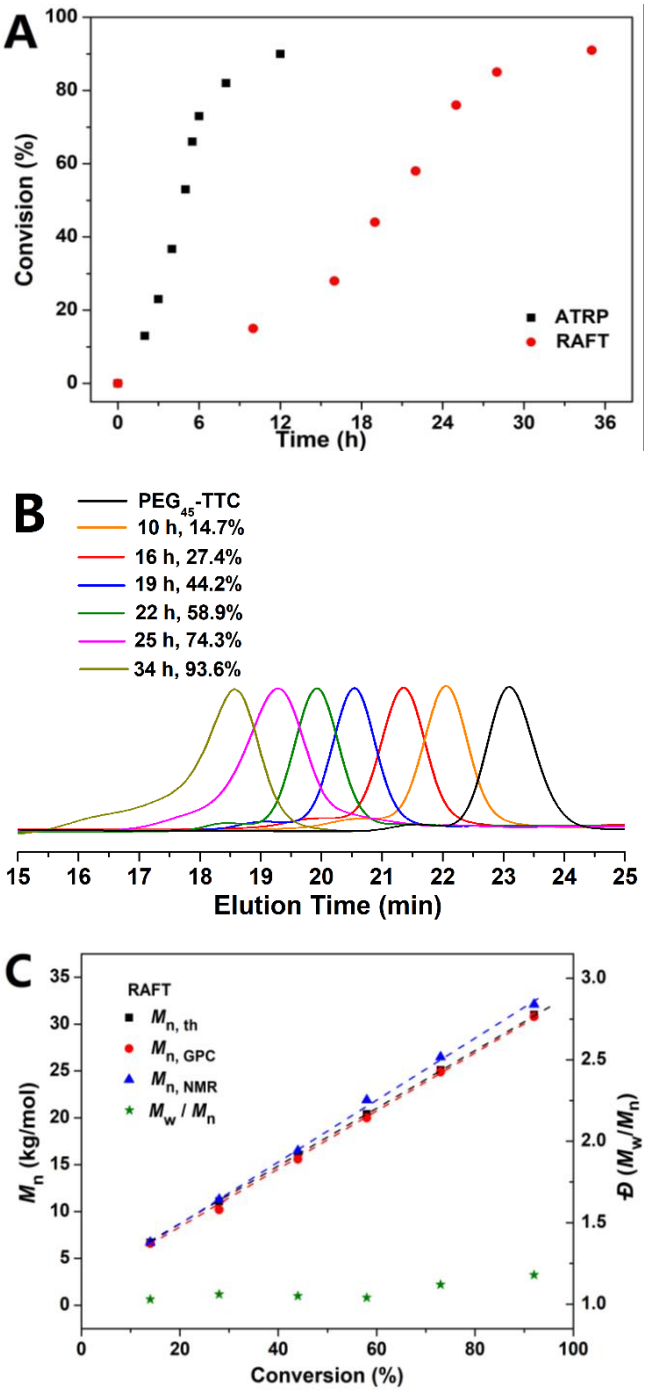

Figure S3. The monomer conversion-time plot for the synthesis of PEG_{45}-*b*-PS by RAFT dispersion polymerization and by ICAR ATRP dispersion polymerization (A), the GPC traces (B), molecular weight and molecular weight distribution (*Đ*) (C) of PEG_{45}-*b*-PS synthesized by RAFT dispersion polymerization.

6. Synthesis and characterization of PEG_{45}-*b*-PS by RAFT dispersion polymerization with excess initiator and $CuBr_2$/TPMA

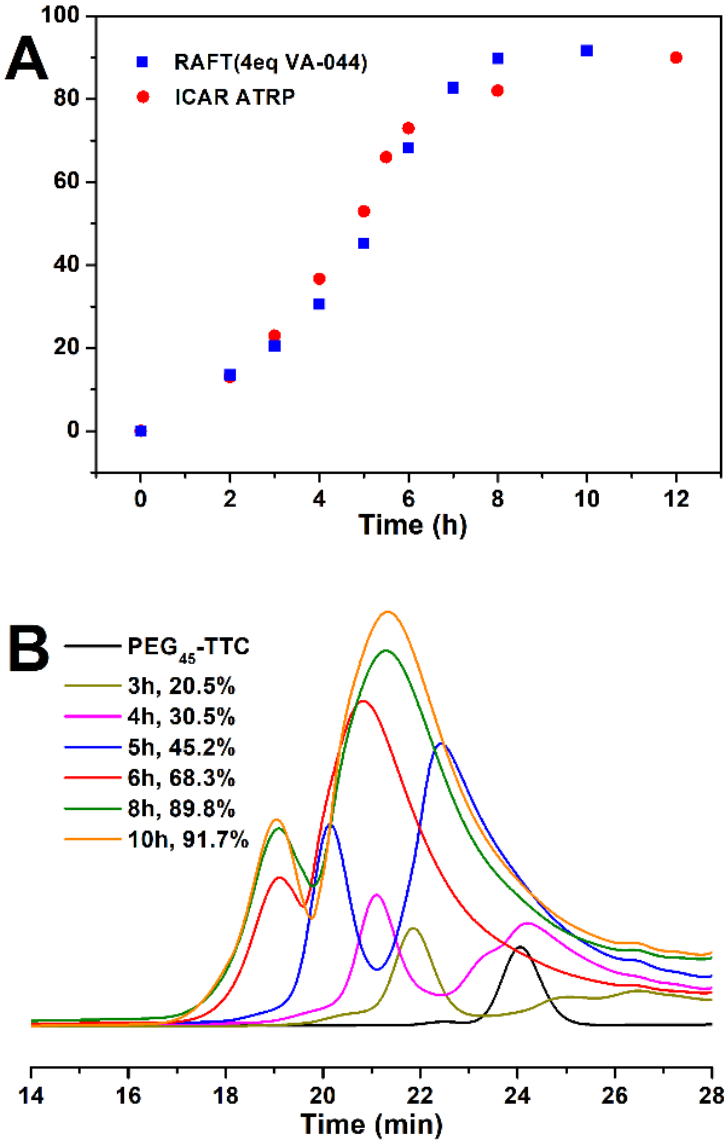

Figure S4. The monomer conversion-time plot (A) for the synthesis of PEG_{45}-*b*-PS by RAFT and ICAR ATRP dispersion polymerization and GPC traces (B) of PEG_{45}-*b*-PS. Polymerization conditions: 20 wt% solid content, 80/20 MeOH/H_2O mixture, 45 ℃, $[St]_0$:$[PEG_{45}\text{-}TTC]_0$:$[VA\text{-}044]_0$:$[CuBr_2]_0$:$[TPMA]_0$ = 300:1:4:0.6:2.4.

The PEG_{45}-*b*-PS nano-assemblies via RAFT dispersion polymerization with excess initiator were synthesized with 20 wt% solid content at 45 ℃ under $[St]_0$:$[PEG_{45}\text{-}TTC]_0$:$[VA\text{-}044]_0$:$[CuBr_2]_0$:$[TPMA]_0$ = 300:1:4:0.6:2.4 in the 80/20 MeOH/H_2O mixture. A typical RAFT dispersion polymerization was introduced

below. Into a 10 mL Schlenk flask, St (0.300 g, 2.90 mmol), PEG_{45}-TTC (0.0226 g, 0.00967 mmol), VA-044 (0.0125 g, 0.0387 mmol), $CuBr_2$ (0.00128 g, 0.00577 mmol), TPMA (0.00670 g, 0.0231 mmol) and 80/20 MeOH/H_2O (1.30 g) were weighed, and the mixture was degassed by three freeze-pump-thaw cycles. Polymerization was performed at 45 ℃ for a given time and then quenched by putting the flask in ice water. The monomer conversion was calculated by UV-vis and nanoparticles were checked by TEM

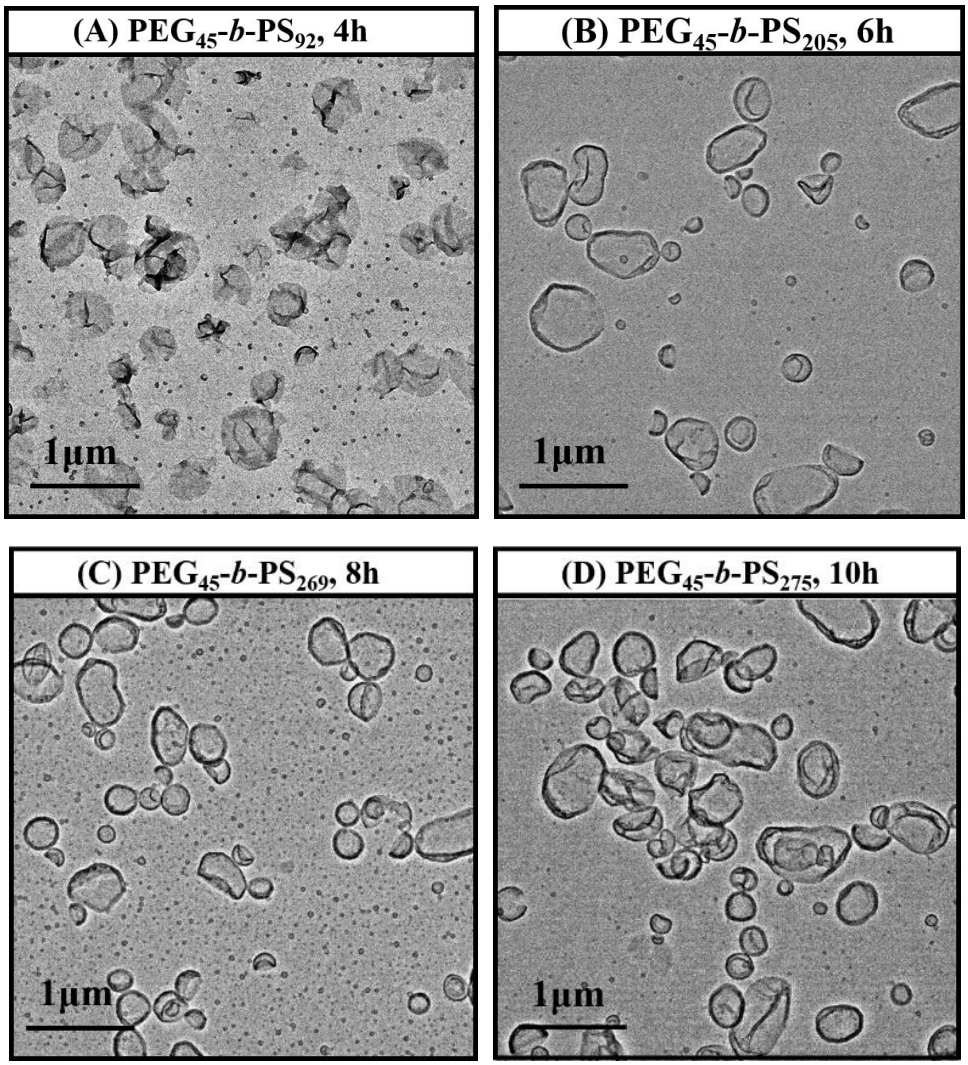

Figure S5. TEM images of the PEG_{45}-*b*-PS nano-assemblies prepared via RAFT dispersion polymerization at 4 h (A), 6 h (B), 8 h (C), 10 h (D). Polymerization conditions: $[St]_0$:$[PEG_{45}\text{-TTC}]_0$:$[\text{VA-044}]_0$:$[CuBr_2]_0$:$[TPMA]_0$ = 300:1:4:0.6:2.4, 45 ℃, 20 wt% solid content in the 80/20 MeOH/H_2O mixture.

7. Solution self-assembly in the presence of $CuBr_2$ and TPMA

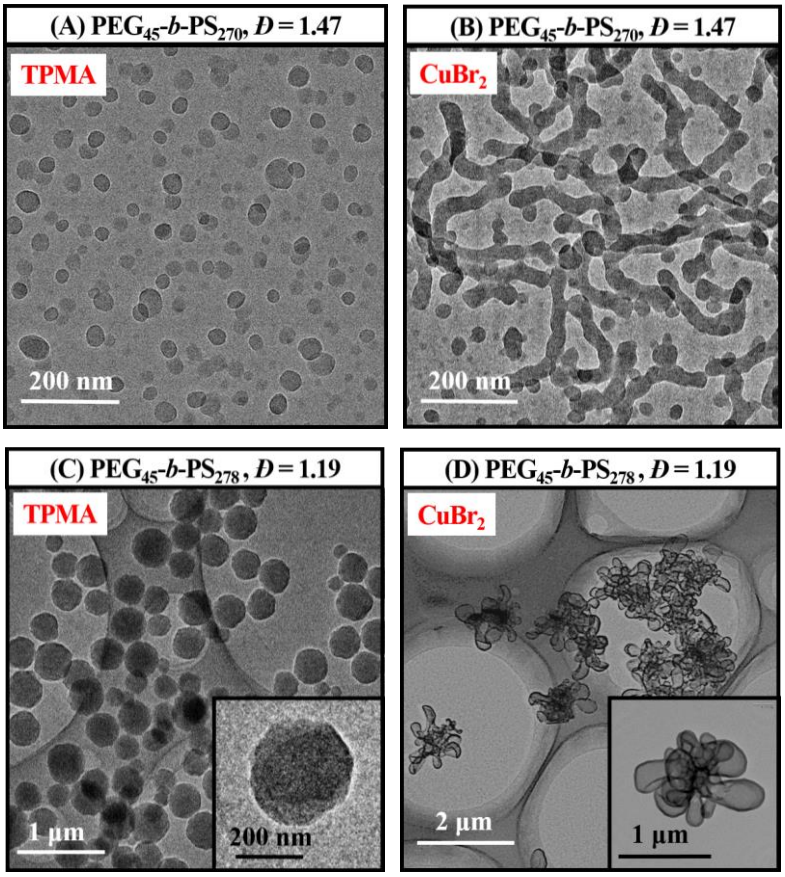

Figure S6. TEM images of the PEG_{45}-*b*-PS (pre-synthesized by ICAR ATRP, *Đ* = 1.47 and RAFT polymerization, *Đ* = 1.19) nano-assembies formed via solution self-assembly in the 80/20 $MeOH/H_2O$ mixture in presence of 2.4 equivalent TPMA (A and C) and in presence of 0.6 equivalent $CuBr_2$ (B and D).

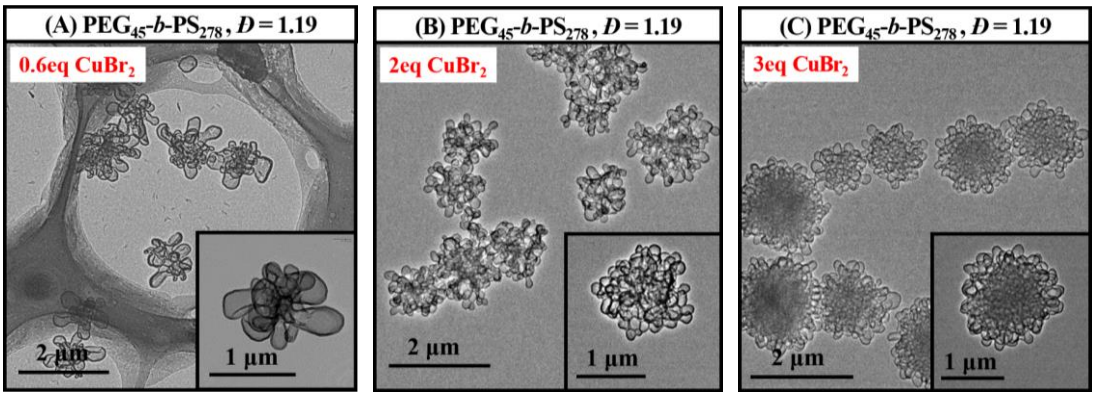

Figure S7. TEM images of the PEG_{45}-*b*-PS_{278} (*Đ* = 1.19) nano-assemblies formed via solution self-assembly in the 80/20 $MeOH/H_2O$ mixture in presence of 0.6 equivalent (A), 2 equivalent (B) and 3 equivalent $CuBr_2$ (C).

8. Synthesis of more BCP nano-assemblies via ICAR ATRP dispersion polymerization

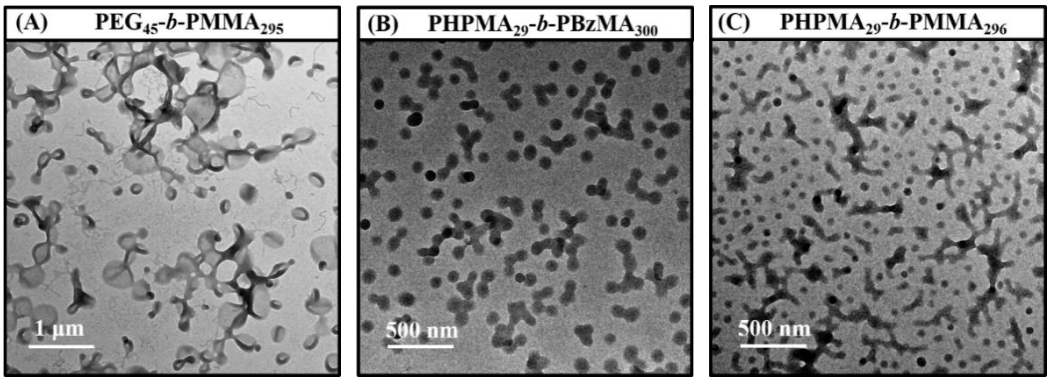

Figure S8. TEM images of the PEG_{45}-*b*-$PMMA_{295}$ (A), $PHPMA_{29}$-*b*-$PBzMA_{300}$ (B) and $PHPMA_{29}$-*b*-$PMMA_{296}$ (C) nano-assemblies prepared via ICAR ATRP dispersion polymerization.